

Reviewer 2:

This is a timely paper that describes the development of a unit-based industrial emission inventory in northern China, which still suffers severe air pollution even though the government has put tremendous amount of effort in emission controls. A detailed, unit-based emission inventory will be of great value when air quality models are used in developing/assessing emission control strategies. The paper is generally well-written. I would recommend the paper be published in ACP after addressing my comments below.

Response: We appreciate the reviewer's valuable comments which help us improve the quality of the manuscript. We have carefully revised the manuscript according to the reviewers' comments. Point-to-point responses are given below. The original comments are in black, while our responses are in blue.

(1) The paper lacks details on how vertical distribution of point source emissions are treated in the simulation. In the results section, it is mentioned that plume rise contributes to the difference between the CMAQ results. However, no details were provided on how the parameters needed for plume rise calculations are obtained. In my understanding, such data are not universally available (even in the US) so presumably the same situation is applicable in China. What is the criteria for selecting point sources for plume rise calculation and how missing information is estimated. I also believe that the authors should perform off-line emission vertical distribution calculations and compare with the empirical vertical distribution used for the proxy-based emission inventory. For many of people without access to the detailed unit-based emission inventory, it will be useful to see this information so that vertical distribution in the traditional inventories can also be improved.

Response:

In the simulation, the vertical distribution of point source emissions is calculated by employing a built-in plume-rise calculation algorithm of CMAQ based on the Briggs's scheme (Briggs, 1982). In this algorithm, plume rise is estimated by simulating the buoyancy effect and momentum rise, using hourly and gridded meteorological data. Then, the plume is distributed into the vertical layers that the plume intersects based on the pressure in each layer. (Page 5, Line 20-22; Page 8, Line 2-4)

The stack information required for plume rise calculation includes stack height, flue gas temperature, chimney diameter and flue gas velocity. For power plants, we get the stack height from Compilation of power industry statistics (China Electricity Council, 2015). For the stack height of cement factories, we refer to the emission standard of air pollutants for cement industry (Ministry of Environmental Protection of China, 2013). For the stack height of glass, brick, lime and ceramics industries, we refer to emission standard of air pollutants for industrial kiln and furnace (Ministry of Environmental Protection of China, 1997). For the stack height of non-ferrous metal smelter, coking, refinery and chemical industries, as well as the flue gas temperature, chimney diameter and flue gas velocity for all industrial sectors, we refer to the national information platform of pollutant discharge permit

(<http://114.251.10.126/permitExt/outside/default.jsp>), where we can find very detailed information of the plants with the pollutant discharge permit. For the sources without the pollutant discharge permit, we use the parameters of the plant with a similar production output or coal consumption. (Page 5, Line 23 to Page 6, Line 5) The data source of stack information is shown in Table R1 (Table S5 in the manuscript).

Table R1 Data source of stack information

Sector	Stack height	Flue gas temperature, Chimney diameter, Flue gas velocity
Power plant	Compilation of power industry statistics	National information platform of pollutant discharge permit

Cement plant	Emission standard of air pollutants for cement industry
Glass, brick, lime and ceramics industries	Emission standard of air pollutants for industrial kiln and furnace
Non-ferrous metal smelter, coking, refinery and chemical industries	National information platform of pollutant discharge permit

The vertical distribution of emissions after plume rise for each industrial sector is shown in Table R2 (Table S6 in the manuscript). The empirical vertical distribution used for the proxy-based emission inventory is also provided for reference (Table R3, Table S7 in the manuscript). In general, compared with the proxy-based inventory, more emissions are distributed in higher vertical levels in the unit-based inventory with plume rise considered.

Table R2 Vertical distribution of emissions for each industrial sector in the unit-based inventory with plume rise considered

Layer	Sigma value	Level height (m)	Power plants		Iron plants		Cement plants		Industrial boilers		Industrial process	
			Jan	Jul	Jan	Jul	Jan	Jul	Jan	Jul	Jan	Jul
1	0.995	35	0%	0%	0%	0%	3%	3%	3%	4%	3%	6%
2	0.99	85	0%	0%	0%	0%	9%	11%	21%	21%	28%	31%
3	0.98	140	0%	0%	0%	6%	26%	32%	32%	41%	45%	36%
4	0.96	210	6%	9%	60%	85%	49%	49%	39%	31%	20%	24%
5	0.94	310	15%	17%	38%	9%	13%	5%	5%	2%	3%	3%
6	0.91	440	47%	45%	2%	0%	1%	0%	0%	0%	0%	0%
7	0.86	610	31%	29%	0%	0%	0%	0%	0%	0%	0%	0%

Table R3 Vertical distribution of emissions for each industrial sector in the proxy-based inventory

Layer	Sigma value	Level height (m)	Power plants	Iron plants	Cement plants	Industrial boilers	Industrial process
1	0.995	35	0%	6%	6%	50%	6%
2	0.99	85	10%	26%	26%	30%	26%
3	0.98	140	10%	68%	68%	20%	68%
4	0.96	210	30%	0%	0%	0%	0%
5	0.94	310	20%	0%	0%	0%	0%
6	0.91	440	20%	0%	0%	0%	0%
7	0.86	610	10%	0%	0%	0%	0%

To separate the contributions of horizontal and vertical distributions to the differences between the simulations using the proxy-based and unit-based inventories, we have conducted an additional simulation in which the unit-based inventory is used but the emission heights are assumed to be the same as the proxy-based inventory. The amount of emission is the same as the other two scenarios. We call the inventory used in this simulation “hypo unit-based inventory”.

Fig. R1 (Fig. 5 in the revised manuscript) shows the distribution of the monthly (January and July) mean concentrations of  $\text{SO}_2$ ,  $\text{NO}_2$ , ozone, daily maximum 1-h averaged ozone, daily maximum 8-h averaged

ozone and PM<sub>2.5</sub> simulated with the proxy-based inventory, and the differences between the proxy-based simulation and the other two simulations (Diff1: hypo unit-based minus proxy-based; Diff2: unit-based minus proxy-based). For SO<sub>2</sub>, NO<sub>2</sub> and PM<sub>2.5</sub>, the concentrations in the urban area are generally higher with the proxy-based inventory than those with the unit-based inventory, especially in winter. In January, large concentration differences between simulations with two inventories are found in urban Tianjin, Tangshan, Baoding and Shijiazhuang, where a large amount of industrial emissions is allocated in the proxy-based inventory due to large population density. The simulation of July follows the same pattern but the concentrations and the difference between the concentrations with two inventories are lower than those of January. In some areas where many factories are located, such as the northern part of Xingtai city, the concentration with unit-based inventory is higher because of a high emission intensity. There are two reasons for the difference between results with proxy-based and unit-based inventories. The first one is the spatial distribution. With detailed information of industrial sectors, more emissions are allocated to certain locations in suburban/rural areas in the unit-based emission inventory. From “Diff1” (hypo unit-based minus proxy-based), we can see that the improved horizontal distribution of the unit-based emission inventory significantly decreases the PM<sub>2.5</sub>, SO<sub>2</sub>, and NO<sub>2</sub> concentrations in most urban centers, and significantly increases the concentrations in a large fraction of suburban and rural areas, especially the areas where large industrial plants are located in. The other reason is vertical distribution. Plume rise is calculated in the simulation with the unit-based inventory, which causes the difference of emissions in vertical layers. The higher the pollutants are emitted, the lower the ground concentration becomes. From the differences between Diff1 and Diff2 we can see that the plume rise leads to lower concentrations over the whole region. The results of the additional simulation have been added to the revised manuscript (Page 11, Line 6 to 26; Page 14, Line 2-4)

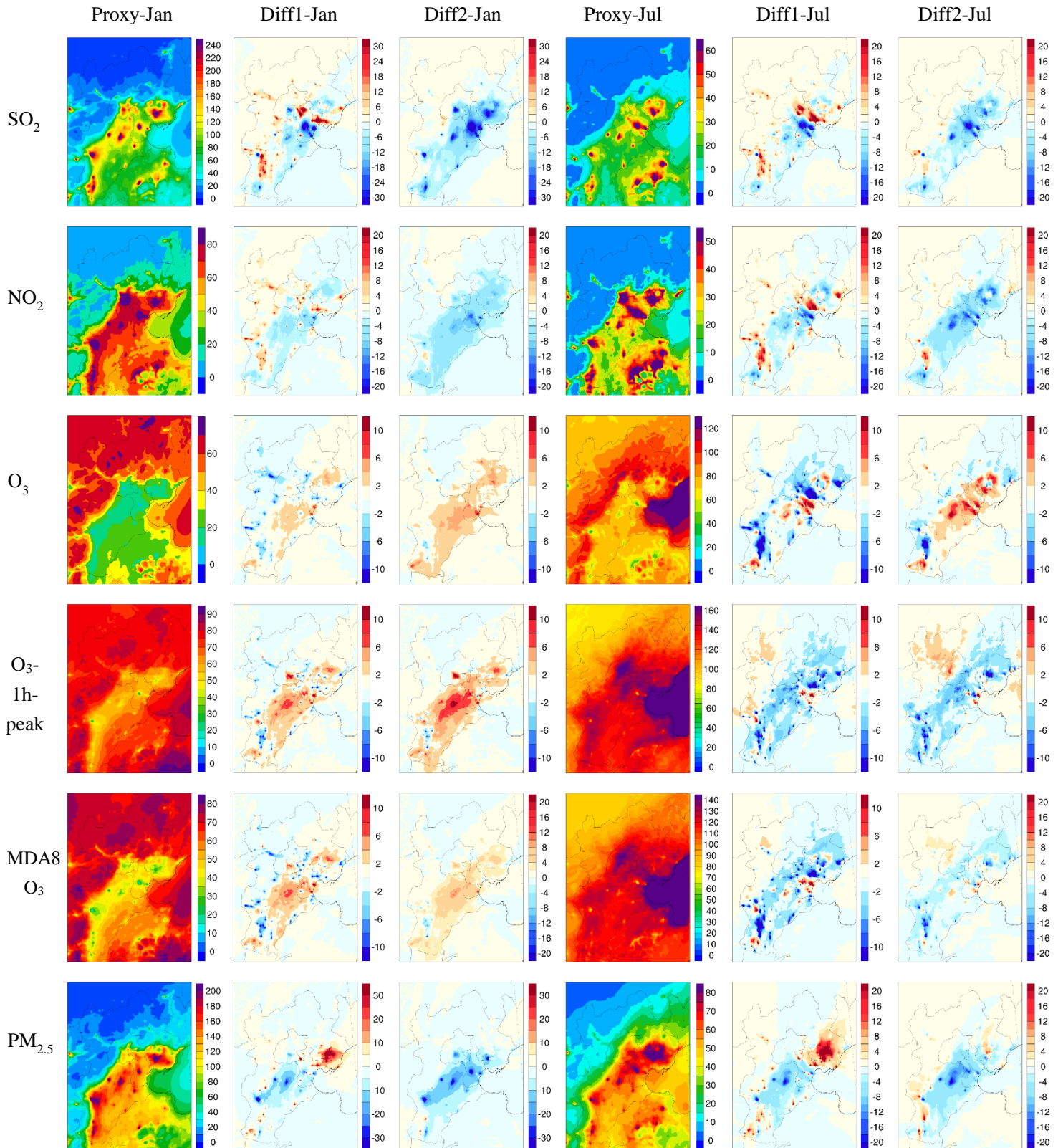


**Fig. R1** Spatial distribution of the monthly (January and July) mean concentrations of SO<sub>2</sub>, NO<sub>2</sub>, ozone, daily maximum 1-h averaged ozone, daily maximum 8-h averaged ozone and PM<sub>2.5</sub> with the proxy-based inventory, and the differences between the other two simulations and proxy-based inventory (Diff1: hypo unit-based minus proxy-based; Diff2: unit-based minus proxy-based). The units are  $\mu\text{g}/\text{m}^3$  for all panels.

(2) One of the major conclusions from the study is that unit-based emission inventory leads to significant improvement in the model performance. However, the only quantitative assessment is monthly average concentrations of SO<sub>2</sub>, NO<sub>2</sub>, O<sub>3</sub>, PM<sub>2.5</sub> using all the stations in the domain. This is not sufficient as information is lost in the averaging process. At minimal, the authors should show performance of these pollutants at each individual sites. Time series should also be shown for sites with significant differences. It will help identify the cause of the differences. For O<sub>3</sub>, it is necessary to show performance of 1-hr peak ozone and 8-hr daily maximum. Very large error still exists for SO<sub>2</sub>. More discussion of this over-estimation should be included.

**Response:**

(1) Following the reviewer's comment, we summarize the model performance for major air pollutants at each individual site in Beijing (12 sites out of a total of 80 sites in the BTH region) in Table R1-R4 (Table S8-S11). The time series of PM<sub>2.5</sub> concentration at representative urban sites (Wanshouxigong and Dongsi) and suburban sites (Huairou and Shunyi) are shown in Fig. R2-R3 (Fig. S7-S8). For the urban sites, the concentrations of PM<sub>2.5</sub>, SO<sub>2</sub> and NO<sub>2</sub> are much lower with the unit-based inventory than with the proxy-based inventory. For the suburban sites, however, the concentrations are either slightly higher or slightly lower with the unit-based inventory than with the proxy-based inventory. The situation for ozone is quite the opposite. The ozone concentration at urban sites is higher with the unit-based inventory than with the proxy-based inventory. In suburban sites, it is lower with the unit-based inventory than with the proxy-based inventory. In addition, for the simulations with the unit-based inventory, the normalized mean error (NME) and mean fractional error (MFE) of individual sites are usually lower than those with the proxy-based inventory while the correlation efficient is usually higher, which means that the error is generally smaller and the trend is more similar to the observation when the unit-based inventory is used.

(2) The figures of time series of PM<sub>2.5</sub> concentration corroborates the preceding conclusion. At urban sites, the concentration with the unit-based inventory is substantially lower than that with the proxy-based inventory throughout the simulation periods. For suburban sites, the concentration is slightly lower with the unit-based inventory than that with the proxy-based inventory in most of the simulation period.

(3) To further quantify the impact of changed emission distribution between urban and suburban areas, we introduced the metric of "concentration gradient", which is defined as the ratios of urban concentrations to suburban concentrations. As shown in Fig. 6 in the manuscript, the concentration gradients simulated with the unit-based inventory agree much better with observations than those simulated with the proxy-based inventory, implying that the unit-based emission inventory better reproduces the distributions of pollutant emissions between the urban and suburban areas.

The preceding tables, figures, and descriptions have been added to the revised manuscript. (Page 12, Line 5-22)

(4) For ozone, the performance statistics for 1-hr peak ozone and 8-hr daily maximum concentration have been calculated, which is shown in Table 2 in the manuscript.

(5) The overestimation of SO<sub>2</sub> concentrations may be due to the lack of several SO<sub>2</sub> reaction mechanisms in CMAQ, such as heterogeneous reactions of SO<sub>2</sub> on the surface of dust particles (Fu et al., 2016), the oxidation of SO<sub>2</sub> by NO<sub>x</sub> in aerosol liquid water (Cheng et al., 2016; Wang et al., 2016), the effects of SO<sub>2</sub> and NH<sub>3</sub> on secondary organic aerosol formation (Chu et al., 2016), etc. The biased

spatial distribution of SO<sub>2</sub> emissions from residential combustion may also contribute to the overestimation. A large fraction of residential combustion takes place in the rural areas. In this work, however, the emission of residential combustion is allocated by GDP and population, which leads to an overestimation of SO<sub>2</sub> emission in urban area and hence an overestimation of SO<sub>2</sub> concentration. (Page 10, Line 4-11)

Table R4 The statistics for model performance of PM<sub>2.5</sub> with proxy-based and unit-based inventories

Months	Sites	Concentration (μg/m <sup>3</sup> )			NMB		NME		MFB		MFE		R	
		proxy-based	unit-based	OBS	proxy-based	unit-based								
Jan	Wanshouxigong	111.2	88.0	108.4	3%	-19%	54%	49%	20%	-3%	62%	60%	0.58	0.60
	Dingling Tomb	36.8	36.9	69.3	-47%	-47%	54%	53%	-59%	-55%	72%	68%	0.67	0.68
	Dongsi	112.2	91.6	104.1	8%	-12%	58%	51%	24%	6%	64%	61%	0.55	0.56
	Heaven Temple	110.7	90.3	97.6	13%	-8%	58%	51%	31%	10%	64%	61%	0.59	0.60
	Nongzhanguan	92.6	77.7	101.9	-9%	-24%	52%	50%	4%	-10%	59%	58%	0.57	0.59
	Guanyuan	110.5	86.4	100.6	10%	-14%	60%	51%	23%	1%	65%	61%	0.55	0.56
	Haidian	86.8	70.0	109.3	-21%	-36%	55%	53%	-17%	-35%	66%	67%	0.53	0.54
	Shunyi	89.4	83.3	92.3	-3%	-10%	56%	54%	8%	3%	62%	61%	0.55	0.55
	Huairou	49.8	48.5	86.9	-43%	-44%	57%	55%	-71%	-69%	86%	82%	0.61	0.62
	Changping	74.7	70.3	85.6	-13%	-18%	54%	51%	-4%	-8%	58%	56%	0.57	0.58
	Olympic center	93.6	82.5	94.8	-1%	-13%	56%	50%	9%	1%	62%	59%	0.57	0.59
	Gucheng	77.0	63.2	102.0	-25%	-38%	50%	51%	-19%	-37%	60%	64%	0.59	0.60
Jul	Wanshouxigong	55.7	50.0	96.4	-42%	-48%	55%	58%	-51%	-61%	69%	75%	0.53	0.52
	Dingling Tomb	24.6	26.1	83.7	-71%	-69%	74%	72%	-106%	-102%	112%	109%	0.55	0.57
	Dongsi	57.3	52.2	110.0	-48%	-53%	57%	59%	-54%	-61%	72%	75%	0.56	0.55
	Heaven Temple	58.0	52.5	103.3	-44%	-49%	56%	58%	-52%	-61%	70%	74%	0.51	0.50
	Nongzhanguan	54.4	50.2	91.7	-41%	-45%	54%	55%	-54%	-59%	70%	72%	0.50	0.50
	Guanyuan	54.8	49.8	99.6	-45%	-50%	55%	57%	-59%	-67%	73%	78%	0.56	0.56
	Haidian	42.8	39.9	99.8	-57%	-60%	61%	63%	-88%	-91%	93%	95%	0.60	0.60
	Shunyi	60.2	55.8	101.7	-41%	-45%	54%	55%	-41%	-47%	67%	70%	0.58	0.57
	Huairou	44.8	45.0	101.2	-56%	-56%	60%	59%	-89%	-78%	96%	85%	0.68	0.68
	Changping	37.2	39.0	91.9	-60%	-58%	65%	63%	-77%	-74%	86%	84%	0.65	0.67
	Olympic center	50.5	47.1	104.8	-52%	-55%	57%	59%	-73%	-77%	81%	83%	0.60	0.59
	Gucheng	38.2	36.9	97.2	-61%	-62%	63%	64%	-96%	-98%	99%	100%	0.64	0.63

Table R5 The statistics for model performance of NO<sub>2</sub> with proxy-based and unit-based inventories

Months	Sites	Concentration (μg/m <sup>3</sup> )			NMB		NME		MFB		MFE		R	
		proxy-based	unit-based	OBS	proxy-based	unit-based								
Jan	Wanshouxigong	135.3	96.0	81.1	67%	18%	81%	47%	43%	11%	59%	46%	0.60	0.64
	Dingling Tomb	39.9	41.4	37.2	7%	11%	60%	58%	4%	11%	60%	60%	0.64	0.66
	Dongsi	135.1	101.4	66.3	104%	53%	116%	75%	59%	37%	72%	60%	0.43	0.42
	Heaven Temple	134.9	101.8	73.4	84%	39%	94%	61%	48%	21%	60%	50%	0.57	0.58
	Nongzhanguan	108.0	93.9	68.0	59%	38%	79%	59%	33%	26%	58%	51%	0.60	0.63
	Guanyuan	141.7	99.9	76.1	86%	31%	103%	61%	42%	12%	63%	52%	0.59	0.59
	Haidian	106.1	80.0	93.5	13%	-14%	66%	50%	-12%	-32%	62%	60%	0.47	0.48
	Shunyi	100.7	92.7	56.8	77%	63%	93%	80%	42%	37%	62%	58%	0.61	0.61
	Huairou	54.8	54.0	56.7	-3%	-5%	72%	68%	-45%	-41%	85%	81%	0.55	0.57
	Changping	102.3	95.3	57.0	80%	67%	98%	87%	39%	34%	60%	57%	0.54	0.56
	Olympic center	113.9	100.0	67.7	68%	48%	86%	66%	43%	37%	63%	58%	0.60	0.62
	Gucheng	95.0	73.6	75.9	25%	-3%	61%	46%	12%	-9%	55%	52%	0.61	0.64
Jul	Wanshouxigong	22.1	18.4	41.3	-46%	-56%	59%	62%	-72%	-86%	83%	92%	0.17	0.15
	Dingling Tomb	5.7	7.2	17.1	-67%	-58%	70%	63%	-116%	-102%	118%	106%	0.34	0.37
	Dongsi	25.6	22.6	43.5	-41%	-48%	57%	58%	-65%	-72%	78%	81%	0.22	0.19
	Heaven Temple	24.5	21.0	36.4	-33%	-42%	56%	56%	-53%	-63%	73%	77%	0.24	0.21
	Nongzhanguan	22.8	21.7	44.9	-49%	-52%	60%	60%	-78%	-77%	87%	84%	0.27	0.27
	Guanyuan	21.4	18.1	42.2	-49%	-57%	61%	62%	-75%	-87%	86%	93%	0.11	0.12
	Haidian	14.9	13.7	54.3	-73%	-75%	74%	76%	-119%	-123%	121%	124%	0.07	0.09
	Shunyi	21.6	19.7	28.1	-23%	-30%	39%	41%	-36%	-43%	54%	57%	0.66	0.64
	Huairou	11.9	12.8	25.0	-52%	-49%	62%	60%	-96%	-86%	105%	95%	0.39	0.40
	Changping	15.1	17.1	32.5	-53%	-47%	58%	54%	-85%	-75%	90%	81%	0.27	0.28
	Olympic center	20.1	18.5	48.6	-59%	-62%	64%	64%	-93%	-96%	97%	99%	0.23	0.25
	Gucheng	12.4	12.2	45.6	-73%	-73%	74%	74%	-118%	-118%	119%	118%	0.23	0.24

Table R6 The statistics for model performance of SO<sub>2</sub> with proxy-based and unit-based inventories

Months	Sites	Concentration (μg/m <sup>3</sup> )			NMB		NME		MFB		MFE		R	
		proxy-based	unit-based	OBS	proxy-based	unit-based								
Jan	Wanshouxigong	102.2	93.4	62.0	65%	51%	77%	67%	60%	51%	69%	65%	0.51	0.51
	Dingling Tomb	36.0	36.7	35.4	2%	3%	73%	71%	-9%	-4%	70%	69%	0.43	0.44
	Dongsi	99.8	91.8	56.7	76%	62%	86%	75%	64%	57%	72%	67%	0.52	0.53
	Heaven Temple	99.7	92.0	47.1	112%	95%	124%	112%	81%	74%	88%	84%	0.30	0.30
	Nongzhanguan	88.0	82.7	58.9	50%	40%	69%	62%	49%	45%	64%	61%	0.50	0.52
	Guanyuan	101.2	91.6	54.8	85%	67%	97%	84%	67%	58%	77%	72%	0.51	0.51
	Haidian	89.7	81.7	58.2	54%	40%	81%	73%	48%	40%	72%	70%	0.47	0.46
	Shunyi	68.9	66.1	44.0	57%	50%	79%	75%	56%	53%	73%	71%	0.48	0.47
	Huairou	46.3	46.5	45.6	2%	2%	66%	63%	-8%	-4%	74%	71%	0.40	0.40
	Changping	66.3	64.0	57.6	15%	11%	58%	56%	12%	8%	56%	56%	0.46	0.46
	Olympic center	87.2	82.6	58.3	50%	42%	72%	66%	45%	42%	65%	62%	0.50	0.50
	Gucheng	80.6	72.4	52.9	52%	37%	79%	69%	47%	38%	71%	66%	0.52	0.52
Jul	Wanshouxigong	69.9	66.5	5.6	1144%	1083%	1168%	1110%	149%	145%	156%	153%	-0.31	-0.31
	Dingling Tomb	9.7	10.5	4.6	112%	128%	168%	178%	52%	58%	97%	98%	0.12	0.11
	Dongsi	74.6	71.8	9.6	680%	650%	696%	669%	135%	133%	141%	141%	-0.05	-0.06
	Heaven Temple	67.3	64.0	7.4	805%	762%	831%	790%	136%	133%	146%	144%	-0.27	-0.28
	Nongzhanguan	62.9	61.0	8.7	622%	600%	649%	627%	127%	128%	137%	138%	-0.07	-0.08
	Guanyuan	77.0	73.5	8.5	802%	761%	842%	802%	149%	147%	155%	153%	0.04	0.04
	Haidian	62.5	60.2	12.2	413%	394%	444%	424%	96%	95%	122%	120%	-0.26	-0.26
	Shunyi	36.8	33.5	6.5	463%	412%	498%	454%	112%	106%	130%	128%	-0.13	-0.15
	Huairou	22.9	23.7	4.5	405%	422%	435%	451%	112%	119%	126%	129%	-0.01	-0.02
	Changping	28.2	30.6	5.4	421%	466%	457%	493%	114%	122%	127%	133%	-0.06	-0.02
	Olympic center	64.2	61.8	5.0	1174%	1127%	1193%	1147%	141%	140%	149%	149%	-0.09	-0.08
	Gucheng	44.1	43.0	5.2	741%	720%	767%	744%	128%	128%	140%	139%	-0.19	-0.17

Table R7 The statistics for model performance of ozone with proxy-based and unit-based inventories

Months	Sites	Concentration ( $\mu\text{g}/\text{m}^3$ )			NMB		NME		MFB		MFE		R	
		proxy-based	unit-based	OBS	proxy-based	unit-based								
Jan	Wanshouxigong	11.0	14.0	12.0	-8%	17%	100%	115%	-86%	-71%	153%	149%	0.43	0.40
	Dingling Tomb	47.2	46.4	35.4	33%	31%	56%	54%	20%	21%	80%	78%	0.60	0.61
	Dongsi	12.0	14.7	23.3	-49%	-37%	71%	75%	-116%	-106%	139%	137%	0.50	0.44
	Heaven Temple	11.5	14.2	20.8	-45%	-32%	76%	82%	-108%	-97%	144%	143%	0.46	0.41
	Nongzhanguan	15.9	17.5	20.9	-24%	-16%	67%	69%	-87%	-80%	128%	127%	0.61	0.59
	Guanyuan	12.6	16.1	16.0	-21%	1%	82%	94%	-78%	-62%	144%	142%	0.50	0.43
	Haidian	18.3	22.8	14.9	23%	54%	99%	122%	-48%	-34%	139%	138%	0.53	0.42
	Shunyi	20.4	21.3	22.9	-11%	-7%	57%	57%	-66%	-59%	116%	113%	0.71	0.70
	Huairou	40.8	40.2	26.2	56%	53%	87%	86%	13%	13%	101%	100%	0.53	0.52
	Changping	26.9	28.1	25.9	4%	9%	55%	55%	-34%	-28%	90%	89%	0.65	0.65
	Olympic center	17.2	18.5	15.6	10%	18%	84%	92%	-50%	-47%	136%	136%	0.58	0.52
	Gucheng	20.6	25.1	31.5	-35%	-20%	64%	65%	-84%	-64%	112%	105%	0.51	0.47
Jul	Wanshouxigong	57.8	58.5	104.8	-45%	-44%	55%	55%	-89%	-86%	104%	102%	0.63	0.62
	Dingling Tomb	106.6	107.4	115.2	-7%	-7%	40%	38%	1%	1%	40%	39%	0.49	0.56
	Dongsi	55.1	55.5	92.8	-41%	-40%	57%	57%	-82%	-80%	104%	102%	0.55	0.54
	Heaven Temple	58.6	59.0	101.3	-42%	-42%	55%	55%	-82%	-78%	102%	99%	0.63	0.61
	Nongzhanguan	63.4	63.1	107.0	-41%	-41%	57%	57%	-58%	-57%	99%	98%	0.56	0.56
	Guanyuan	56.5	57.3	98.7	-43%	-42%	61%	61%	-79%	-77%	107%	105%	0.52	0.52
	Haidian	68.5	69.3	83.4	-18%	-17%	58%	57%	-28%	-26%	93%	92%	0.54	0.55
	Shunyi	70.2	71.2	101.9	-31%	-30%	44%	44%	-37%	-33%	63%	61%	0.70	0.69
	Huairou	92.8	91.1	112.0	-17%	-19%	41%	41%	-12%	-14%	46%	46%	0.54	0.54
	Changping	91.4	90.1	115.3	-21%	-22%	44%	42%	-17%	-18%	52%	51%	0.51	0.55
	Olympic center	64.3	64.7	90.3	-29%	-28%	59%	59%	-45%	-43%	99%	97%	0.52	0.52
	Gucheng	80.5	80.4	100.4	-20%	-20%	51%	50%	-15%	-15%	73%	72%	0.58	0.59

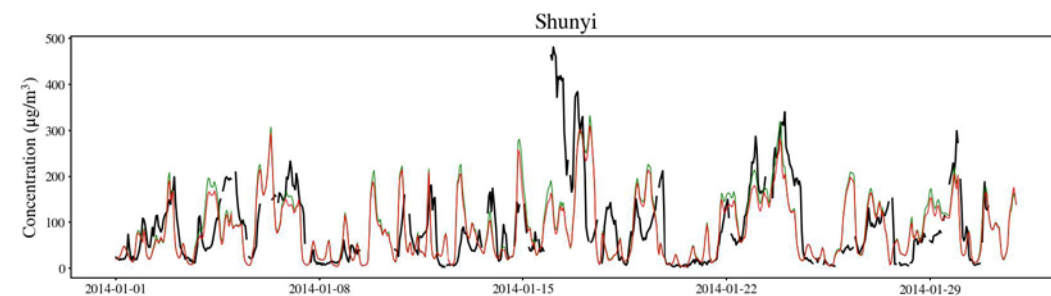
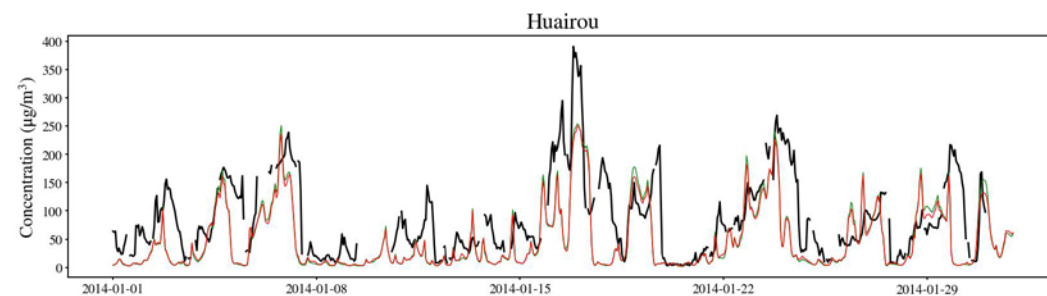
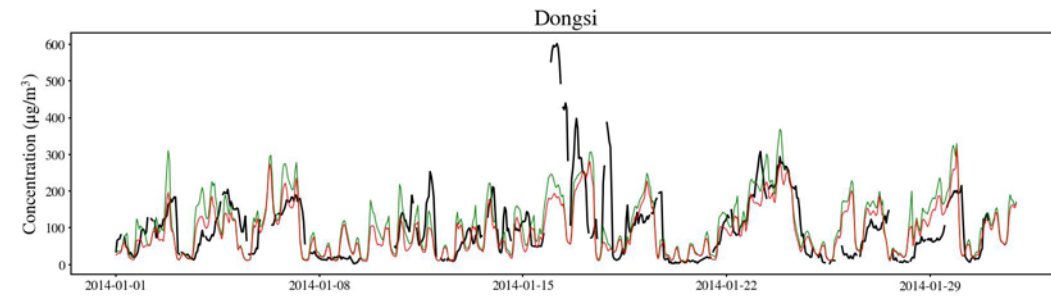
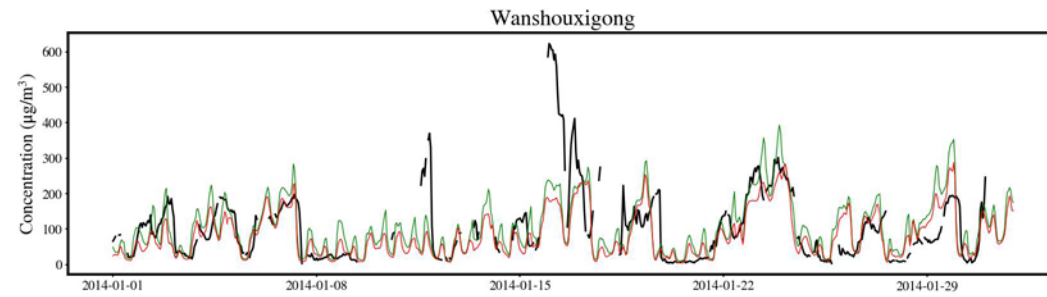


Fig. R2 The PM<sub>2.5</sub> concentration in January in Beijing (The black, green and red lines represent observation, results with proxy-based and unit-based inventories)

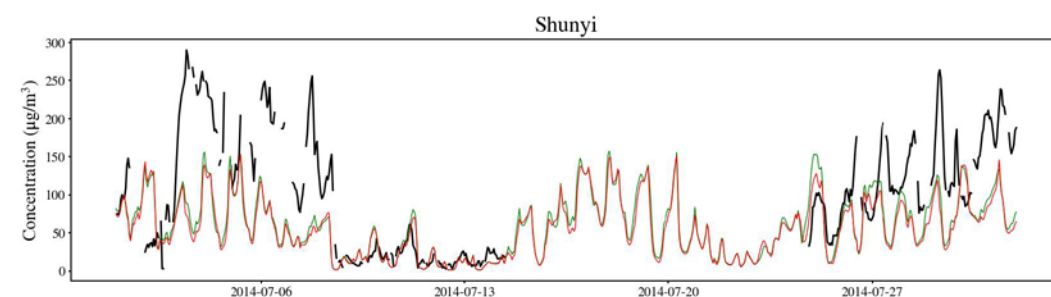
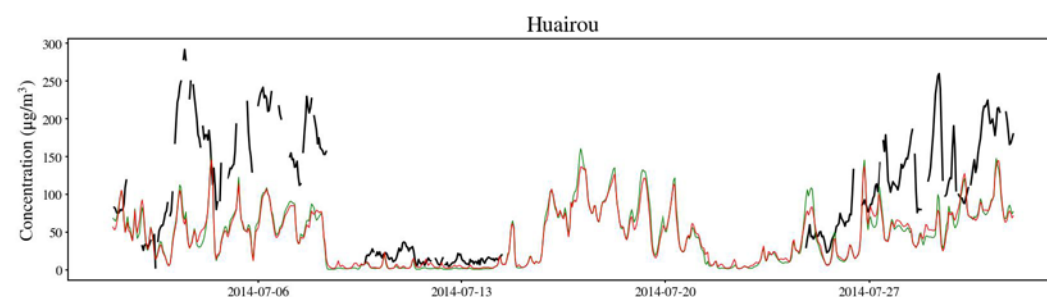
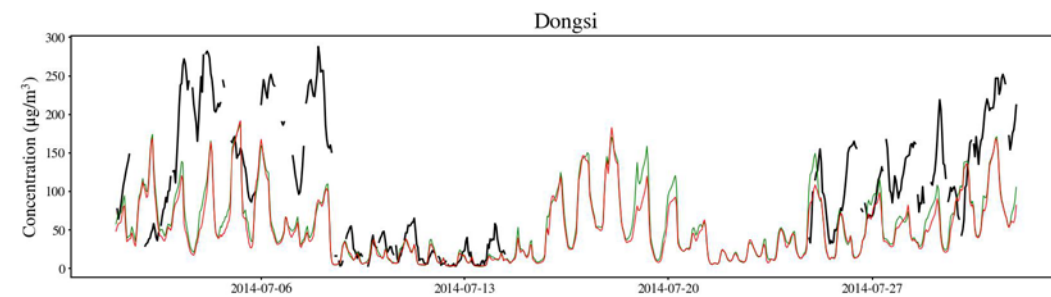
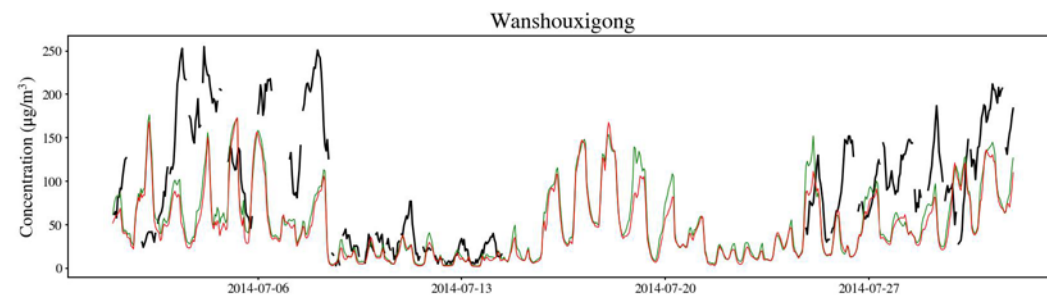


Fig. R3 The PM<sub>2.5</sub> concentration in July in Beijing

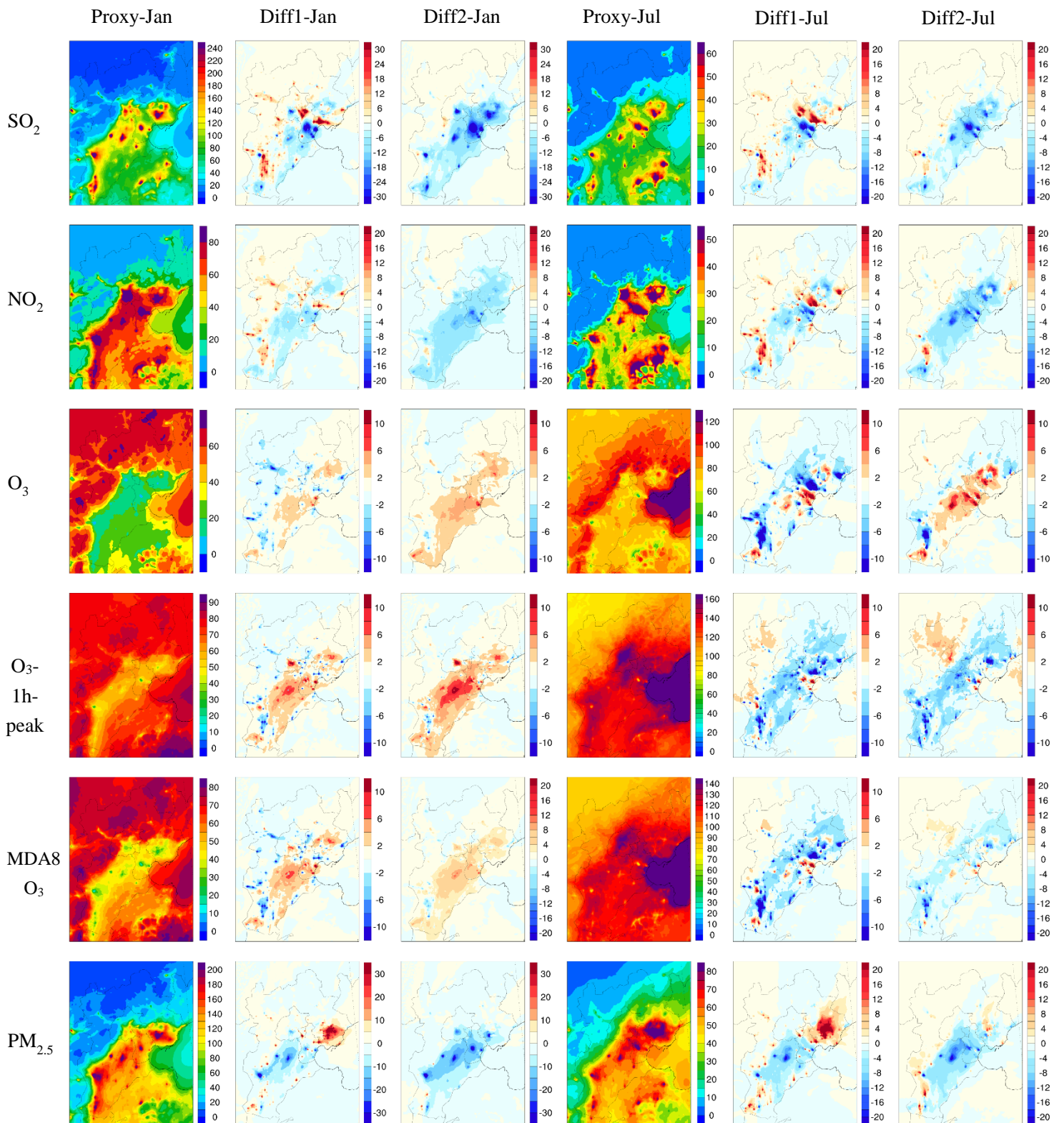


Fig. R4 Spatial distribution of the monthly (January and July) mean concentrations of SO<sub>2</sub>, NO<sub>2</sub>, ozone, 1h-peak ozone, MDA8 ozone and PM<sub>2.5</sub> with the proxy-based inventory, and the differences between the other two simulations and proxy-based inventory (Diff1: hypo unit-based minus proxy-based; Diff2: unit-based minus proxy-based). The units are  $\mu\text{g}/\text{m}^3$  for all panels.

(3) Table 1 shows "annual average" but only January and July simulations were performed. How did you calculate annual average with only two months of simulation?

**Response:** We revised "annual average" to "two-month average" in the revised manuscript. (Table 1)

References:

Briggs, G. A.: Plume Rise Predictions, in: Lectures on Air Pollution and Environmental Impact Analyses, edited by: Haugen, D. A., American Meteorological Society, Boston, MA, 59-111, 1982.

Cheng, Y., Zheng, G., Wei, C., Mu, Q., Zheng, B., Wang, Z., Gao, M., Zhang, Q., He, K., Carmichael, G., Poschl, U., and Su, H.: Reactive nitrogen chemistry in aerosol water as a source of sulfate during haze events in China, *Science Advances*, 2, 10.1126/sciadv.1601530, 2016.

China Electricity Council: Compilation of power industry statistics 2014, China Electricity Council, Beijing, 2015.

Chu, B., Zhang, X., Liu, Y., He, H., Sun, Y., Jiang, J., Li, J., and Hao, J.: Synergetic formation of secondary inorganic and organic aerosol: effect of  $\text{SO}_{2}$  and  $\text{NH}_3$  on particle formation and growth, *Atmos Chem Phys*, 16, 14219-14230, 10.5194/acp-16-14219-2016, 2016.

Fu, X., Wang, S., Chang, X., Cai, S., Xing, J., and Hao, J.: Modeling analysis of secondary inorganic aerosols over China: pollution characteristics, and meteorological and dust impacts, *Sci Rep*, 6, 35992, 10.1038/srep35992, 2016.

Ministry of Environmental Protection of China: Emission standard of air pollutants for industrial kiln and furnace, Ministry of Environmental Protection of China (MEP), Beijing, 1997.

Ministry of Environmental Protection of China: Emission standard of air pollutants for cement industry, Ministry of Environmental Protection of China (MEP), Beijing, 2013.

Wang, G., Zhang, R., Gomez, M. E., Yang, L., Levy Zamora, M., Hu, M., Lin, Y., Peng, J., Guo, S., Meng, J., Li, J., Cheng, C., Hu, T., Ren, Y., Wang, Y., Gao, J., Cao, J., An, Z., Zhou, W., Li, G., Wang, J., Tian, P., Marrero-Ortiz, W., Secrest, J., Du, Z., Zheng, J., Shang, D., Zeng, L., Shao, M., Wang, W., Huang, Y., Wang, Y., Zhu, Y., Li, Y., Hu, J., Pan, B., Cai, L., Cheng, Y., Ji, Y., Zhang, F., Rosenfeld, D., Liss, P. S., Duce, R. A., Kolb, C. E., and Molina, M. J.: Persistent sulfate formation from London Fog to Chinese haze, *Proc Natl Acad Sci U S A*, 10.1073/pnas.1616540113, 2016.